Journal of Pain 45 (2026) 106308

Contents lists available at ScienceDirect

The Journal of Pain

journal homepage: www.jpain.org

Original Reports

Dopamine D_4 receptor activation preserves morphine analgesia and attenuates tolerance by enforcing inhibitory spinal tone in rats

Marina Ponce-Velasco [a,b], M. Ángeles Real [a,b], Adrián Ruiz-Villalba [b,c], Belén Gago [b,d], Iván Fatuarte-Juli [a,b], Mireya Moreno-Ruiz [a], Ismael Aranda-Bravo [a,b], Carolina Roza [e], Alicia Rivera [a,b,*]

[a] Departamento de Biología Celular, Genética y Fisiología, Facultad de Ciencias, Universidad de Málaga, Spain
[b] IBIMA Plataforma Bionand, Instituto de Investigación Biomédica de Málaga, Málaga, Spain
[c] Departamento de Biología Animal, Facultad de Ciencias, Universidad de Málaga, Spain
[d] Departamento de Fisiología Humana, Facultad de Medicina, Universidad de Málaga, Spain
[e] Faculty of Health Sciences, International University of La Rioja (UNIR), Logroño, Spain

ARTICLE INFO

Keywords:
Dopamine D_4 receptor
Morphine
Opioid tolerance
Antinociception
Dorsal horn

ABSTRACT

The clinical efficacy of opioid-based therapies is severely limited by the emergence of maladaptive neuroplasticity which drives both analgesic tolerance and paradoxical pain sensitization. Although these processes involve spinal nociceptive circuits, the endogenous modulatory systems capable of selectively restraining maladaptive plasticity without compromising opioid analgesia, remain incompletely characterized. The dopamine D_4 receptor (D_4R) has been previously shown to constrain morphine-induced neuroadaptations within supraspinal circuits that underlie addiction, positioning it as a compelling candidate to regulate opioid-induced plasticity at the spinal level. Here, we investigated whether D_4R activation modulates spinal mechanisms underlying morphine tolerance and hyperalgesia. Using integrated behavioral, molecular, and neuroanatomical approaches in rats, we show that D_4R activation preserves morphine antinociception while attenuating tolerance and preventing hyperalgesia. This effect is mediated by selective reshaping of dorsal horn circuitry, including modulation of non-peptidergic C fibers afferents, enhancement of catecholaminergic tone, and a shift of the excitatory-inhibitory balance toward inhibition. At the cellular level, D_4R activation attenuates CREB-dependent signaling and reduces neurokinin-1 (NK1) receptor availability in lamina I projection neurons, which constitute the main spinal output to supraspinal nociceptive centers. Together, these findings identify D_4R as a state-dependent modulator of spinal nociceptive circuitry that selectively contains opioid-induced maladaptive plasticity while sparing analgesic signaling. These results extend the regulatory role of D_4R from supraspinal addiction-related circuits to spinal pain pathways, highlighting its potential as a therapeutic target to improve the long-term safety of opioid analgesia.

Perspective: D_4R emerges as a key regulator linking supraspinal addiction-related circuits and spinal nociceptive pathways. By restraining maladaptive plasticity while preserving opioid analgesia, D_4R offers a state-dependent mechanism to prevent tolerance and hyperalgesia. Targeting D_4R could thus provide a novel strategy to enhance the long-term safety and efficacy of opioid therapies.

Introduction

Repeated opioid exposure produces a characteristic dissociation between analgesic efficacy and the progressive emergence of hypersensitivity states.[1] While antinociceptive responses are initially striking, sustained administration precipitates tolerance alongside paradoxical opioid-induced hyperalgesia (OIH) and allodynia.[2] These phenomena reflect the engagement of coordinated neuroadaptive processes that reshape nociceptive circuits, extending beyond mere opioid receptor desensitization. A major site where these adaptations converge is the spinal dorsal horn, where chronic opioid exposure promotes a maladaptive reorganization of local circuitry. This remodeling is

* Correspondence to: Departamento de Biología Celular, Genética y Fisiología, Facultad de Ciencias Universidad de Málaga, Campus de Teatinos s/n, Málaga 29071, Spain.
E-mail address: arivera@uma.es (A. Rivera).

https://doi.org/10.1016/j.jpain.2026.106308
Received 17 February 2026; Received in revised form 9 April 2026; Accepted 1 May 2026
Available online 5 May 2026

characterized by a shift in the excitatory-inhibitory balance driven by enhanced glutamatergic excitability,[3] and increased pro-inflammatory signaling.[4]

Spinal lamina I neurokinin-1 receptor-expressing (NK1+) projection neurons constitute a major output pathway conveying nociceptive information to supraspinal centers.[5] Evidence from selective NK1+ projection neuron ablation, pharmacological blockade, or genetic silencing demonstrates that these neurons are essential for the full expression of hypersensitive pain behaviors.[6–8] Under physiological conditions, spinal inhibitory tone tightly constrains NK1+ projection neuron excitability. However, chronic opioid exposure disrupts this regulation, promoting a hyperexcitable state in which NK1+ projection neurons aberrantly engage supraspinal centers.[8,9] Subsequent feedback via descending facilitatory pathways establishes a maladaptive spino-bulbo-spinal loop that contributes to both the development and maintenance of opioid-induced hyperalgesia and tolerance.[10]

While significant research has focused on the mechanisms driving spinal sensitization, it remains unclear whether endogenous neuromodulatory systems can selectively constrain these adaptations without compromising opioid-mediated analgesia. Identifying such regulatory mechanisms is essential for uncoupling opioid efficacy from its long-term liabilities. Descending monoaminergic systems exert potent control over spinal nociceptive processing.[11,12] However, whereas noradrenergic and serotonergic pathways have been extensively characterized, dopaminergic modulation remains comparatively poorly understood, particularly in the context of opioid-induced plasticity.[12] Spinal dopamine signaling exerts a complex, bidirectional influence on nociception through the opposing actions of D1- and D2-like receptors. While activation of D1-like receptors typically promotes pro-nociceptive states,[13] the D2-like receptors predominantly mediate antinociceptive effects.[14] Despite these insights, the specific functional contribution of individual receptor subtypes within these families remains largely unresolved, limiting our ability to determine whether discrete dopaminergic targets can differentially regulate opioid analgesia and maladaptive plasticity.

The dopamine D_4 receptor (D_4R) emerges as a compelling candidate for modulating spinal opioid-induced neuroplasticity. In supraspinal circuits, D_4R has been shown to constrain the molecular and cellular adaptations associated with opioid-related habit formation and the consolidation of addiction.[15–18] Given its expression within the dorsal horn,[19] and its well-established inhibitory role in C-fiber nociceptors,[20] we hypothesized that selective activation of D_4R could regulate the maladaptive spinal plasticity underlying opioid-induced sensitization and the progressive loss of analgesic efficacy. Through selective pharmacological activation, D_4R was targeted to assess its ability to modulate excitatory-inhibitory balance, dorsal horn circuitry, and nociceptive output under morphine administration.

Methods

Animals

Adult male Sprague-Dawley rats (Janvier Labs, Le Genest-Saint-Isle, France), weighing 180–200 g at the beginning of the experiments, were housed in standard conditions (22 ± 2 °C room temperature, 55–60% relative humidity) with environmental enrichment and a 12 h light/dark cycle including simulated dawn/dusk transitions. Tap water and standard rodent chow were available *ad libitum*. Animal care and experimental procedures complied with the European Union Council Directive (2010/63/EU) and Spanish Government regulations (RD 53/2013), and were approved by the Ethical Committee of the University of Málaga (CEUMA 79–2019-A). All animal experiments were designed and reported in accordance with the ARRIVE guidelines. The number of animals used and their suffering were minimized in accordance with the 3Rs principles. Experiments were conducted exclusively on male rats to maintain consistency with our previously published results.[15,16] The potential influence of sex as a biological variable is addressed in the Discussion. No animals were excluded from data analysis.

Drug treatments

Morphine sulfate was obtained from Alcaliber S.A. (Madrid, Spain) following authorization from the Spanish Agency of Medicines and Medical Devices (Spanish Government). PD168,077 maleate (D_4R agonist) and L745,870 (D_4R antagonist) were supplied by Tocris Bioscience (Bristol, UK). All drugs were dissolved in a vehicle solution consisting of 0.9% NaCl and 2% DMSO. DMSO was required due to the low aqueous solubility of PD168,077, following manufacturer recommendations. Previous work from our laboratory confirmed that this vehicle solution does not affect receptor function.[21]

The dose of PD168,077 (1 mg/kg) was selected based on its demonstrated efficacy in counteracting cellular, molecular, and behavioral effects of morphine in addiction-related paradigms.[15,16] The morphine dose (7 mg/kg) was determined in a pilot study showing maximal acute analgesic effect and induction of antinociceptive tolerance following daily administration for 8 consecutive days (Supplementary Figure S1A-B).

Animals were randomly assigned to treatment groups to receive vehicle, morphine, PD168,077, L745,870, or morphine + PD168,077. Experimenters were blinded to the identity and experimental conditions of the animals and tissues. Treatments were administered intraperitoneally (i.p.) once daily for 8 consecutive days. Sample sizes (n) for each experiment were determined based on prior experience with similar protocols.

Anti-nociception assessment

To assess the impact of D_4R activation on morphine-induced analgesia and tolerance development, nociceptive responses to thermal (tail flick test) and mechanical (von Frey test) stimuli were measured. Rats were habituated to the testing procedures for two consecutive days prior to experimental assignment. Baseline measurements were obtained 30 min before the first drug administration. Antinociceptive effects were evaluated on the first (acute) and eighth (chronic) days of treatment.

Tail flick test

The tail flick test was performed using a tail flick apparatus (LE106, Panlab, Barcelona, Spain) following previously described procedures.[15] Rats (n = 8–12 per group) were restrained to limit mobility, with their tails positioned on the apparatus platform. A halogen lamp beam was directed at the dorsal surface of the tail, and the withdrawal latency was recorded. Stimulus intensity was adjusted to achieve baseline latencies of 3–5 s. To prevent tissue damage, a cut-off of 15 s was imposed. Latency was measured at 30-min intervals for 150 min following treatment administration. The time course of the thermal antinociceptive response for each drug treatment was plotted as the percentage of antinociception, calculated using the following formula: % antinociception = [(test response time – basal response time) / (cut-off time - basal response time)] x 100. Overall antinociception, encompassing both magnitude and duration, was assessed by calculating the area under the curve (AUC).

von Frey test

The von Frey test was conducted using the ascending force paradigms[22] to determine the paw withdrawal threshold of animals. Rats (n = 8–11 per group) were individually placed in transparent plastic chambers (17-cm long x 22-cm wide x 14-cm high) on a wire grid platform and allowed to habituate for at least 30 min. The mid-plantar surface of the hind paw was stimulated using a series of eight von Frey filaments (Ugo Basile, Gemonio, Italy; calibrated forces ranging from 1.4 to 26.0 g) applied perpendicularly from beneath the mesh floor. The experimental cut-off was set at 26.0 g. Starting with the lowest force

filament, each filament was applied five times with 1-min intervals. In the absence of paw withdrawal response, the next filament in ascending order of force was presented. This process continued until paw withdrawal occurred in 40% of the trials. The time course of mechanical antinociception was measured at 30-min intervals for 150 min post-administration and plotted as the percentage of antinociception, calculated with the formula: % antinociception = [(test threshold – basal threshold) / (cut-off filament - basal threshold)] x 100. Overall mechanical antinociception was also assessed as the AUC.

Immunostaining

Spinal cord tissue was collected from a subset of rats (n = 3–7 per treatment group) previously subjected to the tail flick test. Animals were sacrificed either 90 min (for double immunofluorescent labeling) or 4 h (for single immunohistochemical staining) after the final drug administration on day 8. Rats were anesthetized with sodium pentobarbital (60 mg/kg, i.p.) until loss of reflexes, and perfused transcardially with 0.1 M phosphate buffered saline (PBS, pH 7.4). Spinal cords were extracted via hydraulic extrusion, post-fixed in 4% paraformaldehyde for 24 h, cryoprotected with a solution of 30% sucrose in PBS for 72 h, and then frozen in dry ice. Lumbar spinal cord segments (L4–6) were coronally sectioned at 30 μm thickness using a freezing microtome (CM 1325, Leica, Wetzlar, Germany) and collected as free-floating sections for subsequent immunostaining.

Details regarding the primary and secondary antibodies used are listed in Table 1 and Supplementary Table S1, respectively. Optimal concentrations of primary antibodies were determined empirically to enable semi-quantitative evaluation of immunolabeling[21] and to identify double-labeled neurons. To ensure staining consistency, sections from all experimental groups were processed simultaneously using the same reagent batches.

For single antigen immunohistochemistry, sections were processed for standard avidin-biotin peroxidase methods following a previously described protocol.[23] Peroxidase activity was developed with 0.05% 3, 3'-diaminobenzidine (DAB, Sigma-Aldrich, St. Louis, MO, USA), 0.08% nickel ammonium sulfate and 0.02% H_2O_2. Immunostained sections were mounted on gelatin-coated slides, air dried, dehydrated through grade alcohols, and coverslipped using DPX mounting medium.

Double antigen immunolabeling for P-CREB (phosphorylated cAMP response element-binding protein) in combination with NK1 receptor, calbindin (CB), calretinin (CR), or parvalbumin (PV) was performed as previously described.[16] NK1 staining was revealed using an indirect method with a biotinylated secondary antibody and streptavidin-conjugated Alexa 594, whereas P-CREB, CB, CR and PV were directly labeled with appropriate Alexa 647- or Alexa 488-conjugated secondary antibody. Sections were mounted on glass slides, coverslipped with aqueous-based mounting medium, and imaged using a Leica Sterallis DMi8 confocal microscope.

Table 1
Primary antibodies list.

Primary antibodies	Host	Source	Dilution
Calbindin (CB)	mouse	Sigma Aldrich	1:50,000 (IMQ)
Calbindin (CB)	rabbit	Swant	1:5000 (IF)
Calcitonin gene-regulated peptide (CGRP)	mouse	Merk	1:100,000 (IMQ)
Calretinin (CR)	goat	Swant	1:20,000 (IMQ) / 1,5000 (IF)
Mu opioid receptor (MOR)	rabbit	Calbiochem	1:10,000 (IMQ)
Neurokinin-1 receptor (NK1)	guinea pig	Merk	1:5000 (IMQ) / 1:3000 (IF)
Parvalbumin (PV)	mouse	Sigma Aldrich	1:5000,000 (IMQ)
Parvalbumin (PV)	rabbit	Inmunostar	1:5000 (IMF)
Phospho-CREB (P-CREB)	mouse	Santa Cruz	1:750 (IF)
Substance P	rabbit	Inmunostar	1:6000 (IMQ)
Vesicular GABA transporter (vGAT)	mouse	Synaptic Systems	1:5,000 (IMQ)
Vesicular glutamate transporter 2 (vGluT2)	guinea pig	Synaptic Systems	1:100,000 (IMQ)
Lectin IB4 biotinylated		Vector Laboratories	1:10,0000 (IMQ)

Abbreviations: IMQ: immunohistochemistry; IF: immunofluorescence.

Semi-quantitative evaluation of immunoreactivity

Immunoreactivity (IR) in the neuropil (CGRP, calcitonin gene-related peptide; MOR, mu opioid receptor; SP, substance P; vGluT2, vesicular glutamate transporter isoform 2; vGAT, vesicular GABA transporter), neuronal somata/dendrites (CB, CR, PV, NK1), and axonal varicosities (TH, tyrosine hydroxylase), as well as isolectin B4 (IB4) binding, was semi-quantified by measuring optical density (OD) using ImageJ software (version 1.53k, NIH). For P-CREB-, CB-, CR-, and PV-positive neurons, nuclear/cell density (number of nuclei/cells per mm^2) was also determined. For each animal, a minimum of five lumbar dorsal horn sections were analyzed to ensure reliable data acquisition. Grayscale photomicrographs were captured with a VC50 digital camera mounted on an Olympus VS120 optical microscope (Hamburg, Germany) at appropriate magnifications (10x, 60x, or 100x objectives). OD values were background-corrected using measurements from an immunohistochemically negative region. Data were expressed as mean percentage OD relative to the vehicle-treated control group across the entire superficial dorsal horn; lamina I and lamina II were subsequently analyzed separately to assess the relative distribution of each marker. For TH IR varicose terminal-like fibers, morphological features (area and circularity) were assessed. Data were collected from a minimum of 10 clearly focused fibers (each containing five to nine varicosities) per section.

For double immunofluorescence experiments, the proportion of NK1-, CB-, CR-, and PV-positive neurons co-expressing P-CREB was quantified and expressed relative to the total number of each respective neuronal population.

High-performance liquid chromatography (HPLC) analysis

Rats (n = 5 per treatment), previously subjected to the von Frey test, were sacrificed by decapitation 1 h after the final drug injection, following 8 days of daily administration of vehicle, morphine, and/or PD168,077. The L4–6 segments of the lumbar spinal cord were dissected as described above, and the dorsal portion was isolated for subsequent homogenization, metabolite extraction, and quantification of the aminoacids glutamate, GABA, and glycine. Briefly, each dorsal spinal cord extract was homogenized in 5% perchloric acid and centrifuged at 15000 rpm for 10 min. The resulting pellets were washed, resuspended in 1 N NaOH, and subjected to total protein quantification using the Qubit protein assay (Thermo Fisher Scientific, Waltham, MA, USA) to normalize neurotransmitter levels. The supernatant was incubated (70 °C, 45 min) with a derivatizing reagent consisting of a dansyl chloride solution (3 mg/mL 5-dimethylaminonaphthalene-1-sulfonyl chloride in acetonitrile), an internal standard (0.04 nM α-aminoisobutírico in 5% perchloric acid), and 0.1 M sodium hydrogencarbonate buffer (pH 9). HPLC analyses were performed using an Ultimate 3000 UHPLC-Dionex (Thermo Fisher Scientific), equipped with a reverse-phase AcclaimTM 120–18 column (3 μm 4.6 x 100 mm; Thermo Fisher Scientific). Standard curves were generated using known concentrations of glutamate, GABA, and glycine. Chromatographic data were processed using Chromeleon 7 Software (Thermo Fisher Scientific). Neurotransmitter levels were expressed as nanograms per milligram of total protein.

RNA isolation and quantitative polymerase chain reaction (qPCR)

Spinal cord segments (L4–6) and the cerebral cortex were collected from a subset of rats (n = 5 per treatment) previously subjected to the tail flick test. Animals were sacrificed by decapitation 4 h after the final

drug administration on day 8. Total RNA was extracted using E.Z.N.A total RNA kit II (Omega Bio-tek, Norcross, GA, USA) following the manufacturer's recommendations. RNA purity (260/280 ratio $\geq$ 1.8) and concentration were measured using the Nanodrop One spectrophotometer (Thermo Fisher Scientific). Total RNA was stored at -80 ºC. Prior to cDNA preparation, genomic DNA was removed by DNAse treatment (Thermo Fisher Scientific). cDNA synthesis was performed using 500 ng of total RNA per sample using the iScript™ cDNA Synthesis Kit (Bio-Rad, Hercules, CA, USA).

Primers (Table 2) were designed using Primer-Blast (GeneBank, National Centre for Biotechnology Information, Bethesda, MD, USA) based on rat nucleotide sequences from the NCBI Nucleotide database, and validated with Oligoanalyzer v3.1 (Integrated DNA Technologies, Coralville, IA, USA).

qPCR reactions contained cDNA equivalent to 5 ng of initial RNA, 0.5 μM final concentration of forward and reverse primers, and FastStart Essential DNA Green Master mix (Roche, Basel, Switzerland). Amplification was performed on a LightCycler 96 instrument (Roche) using the following protocol: 95 °C for 5 min, followed by 45 cycles of 95 °C for 10 s, 60 °C for 20 s, and 72 °C for 20 s. Product specificity was confirmed by melting curve analysis (LightCycler480, Roche) and size fractionation by 3% agarose gel electrophoresis (Supplementary Figure S2A-C).

To ensure precise quantification in the qPCR experiments, a stability analysis of reference genes was performed. Several candidate (*Eef1e1*, *Hprt1*, *H2az1*, *Pgk1*, *Pppia*, *Rpl13a*, *Tbp*) were selected as potential reference genes based on previous studies,[24] and their stability was evaluated across the combination of eight experimental conditions, including drug treatment and tissue sample types, as previously described.[24] This analysis identified *Eef1e1* and *Tbp* as the most suitable combination of reference genes.

Data from amplification curves were exported to *LinRegPCR* program to determine PCR efficiency and initial cDNA quantity (N0). N0 values were normalized using the geometric mean of the two selected reference genes for each sample. Systematic differences between runs were corrected using the *Factor-qPCR* program.

Statistical analysis

Data are presented as mean ± SEM. Statistical comparisons were performed using Student's *t-test*, one-way or two-way analysis of variance (ANOVA) followed by Bonferroni *post hoc* test (parametric data) or Kruskal-Wallis analysis followed by Dunn's *post hoc* test (nonparametric data). Two-way repeated-measures ANOVA was applied when the same animals were measured repeatedly over time. Statistical significance was set at $p < 0.05$. All analyses were conducted using SigmaStat 3.5 software (Systat Software, San Jose, CA, USA).

Results

D_4R activation attenuates morphine-induced antinociception tolerance and hyperalgesia

To investigate the influence of D_4R on morphine-induced antinociception and tolerance development, behavioral responses to thermal and mechanical stimuli were evaluated using the tail flick and von Frey tests, respectively, following acute and chronic (8-day) drug administration. Consistent with previous findings,[15] neither acute nor chronic administration of the D_4R agonist PD168,077 elicited detectable nociceptive effects (Fig. 1A-B, A'-B'). In contrast, chronic D_4R blockade with the selective antagonist L745,870 induced mechanical allodynia in the von Frey test (Fig. 1B').

Acute co-administration of PD168,077 with morphine produced an antinociceptive time-course comparable to morphine alone in both assays (Fig. 2A, B), characterized by peak analgesia between 30- and 60-min post-injection, followed by a gradual decline over 150 min. Notably, in the von Frey test, D_4R activation prolonged the duration of morphine's analgesic effect, with antinociception remaining significantly higher (by ~25%) at the 120-min time point compared to morphine alone (Fig. 2B).

After 8 days of chronic treatments, rats receiving morphine alone exhibited pronounced tolerance, evidenced by a substantial reduction in analgesic efficacy (Fig. 2A', B'). This effect, consistently observed in both the tail flick and von Frey assays, was markedly attenuated by co-administration of morphine + PD168,077 (Fig. 2A', B'). Comparison of overall treatment effectiveness through AUC calculation further supported these findings. Chronic morphine administration led to a substantial reduction in AUC compared to the acute treatment (~70% decrease in tail flick, Fig. 2A''; ~48% decrease in von Frey, Fig. 2B''), indicative of tolerance development. In contrast, chronic co-administration of morphine + PD168,077 produced a significantly smaller reduction in AUC (~40% decrease in tail flick, Fig. 2A''; ~25% decrease in von Frey, Fig. 2B'').

We next investigated the role of D_4R in modulating morphine-induced peripheral sensitization and associated sensory alterations. Our results show that chronic morphine exposure significantly triggered thermal hyperalgesia, which was completely prevented by the co-administration of the D_4R agonist (Fig. 3A). No significant mechanical allodynia was observed (Fig. 3B).

Collectively, these findings indicate that D_4R activation does not interfere with acute morphine analgesia but effectively attenuates tolerance development and prevents morphine-induced thermal hyperalgesia following chronic administration.

Chronic D_4R activation during morphine treatment does not alter spinal expression of opioid or D2-like dopamine receptors

Previous studies indicate that selective activation of D_4R can modulate MOR expression and signaling within the rat caudate putamen,[18,21] contributing to the antagonistic effects of D_4R activation on morphine-induced addiction.[15] Given the well-established role of opioid receptors in morphine analgesia[25] and our observation that D_4R activation attenuates the development of tolerance to morphine, we hypothesized that D_4R could influence opioid analgesic efficacy, potentially through the regulation of opioid receptor genes expression. To test this, we examined mRNA expression levels of MOR, DOR (delta opioid receptor), and KOR (kappa opioid receptor) in the dorsal horn following chronic treatment. qPCR analysis revealed no significant changes in *Oprm1* (MOR; Fig. 4A), *Oprd1* (DOR; Fig. 4B), or *Oprk1* (KOR; Fig. 4C) mRNA levels compared to vehicle controls.

Since MOR protein distribution exhibits laminar specificity, with

Table 2
PCR primers and amplicon information.

Gene	Accession number	Description	Sequence (5' to 3')	Amplicon (bp)
Drd2	NM_001409379	Dopamine D_2 receptor	FW: AGACACCACTCAAGGGCAACRV: CGCCTGTTCACTGGGAAACT	94
Drd4	NM_012944	Dopamine D_4 receptor	FW: CATCAGCGTGGACAGGTTTGRV: GACAGGGCAGGAAGAAGGAA	227
Eef1e1	NM_001106106.1	Eukaryotic translation elongation factor 1 epsilon 1	FW CAGACTCTGCTGAAGGATCTCARV: AATGTGGCAAAACCAGCGAG	174
Oprd1	NM_012617.1	Delta opioid receptor (DOR)	FW: GGTCTTGGCTTCAGGTGTTGRV: ACGGTGATGATGAGAATGGGC	173
Oprk1	NM_001318742.1	Kappa opioid receptor (KOR)	FW: TGGTGTTTGTGGTGGGCTTARV: GCACTCTGGAAGGGCATAGT	148
Oprm1	NM_001038597.2	Mu opioid receptor (MOR)	FW: GCCATCGGTCTGCCTGTAATRV: GGAGAACGTGAGGGTGCAAT	77
Tbp	NM_001004198.1	TATA box binding protein	FW: GCACAGGAGCCAAGAGTGAARV: CTGAACTGCTGGTGGGTCAA	181

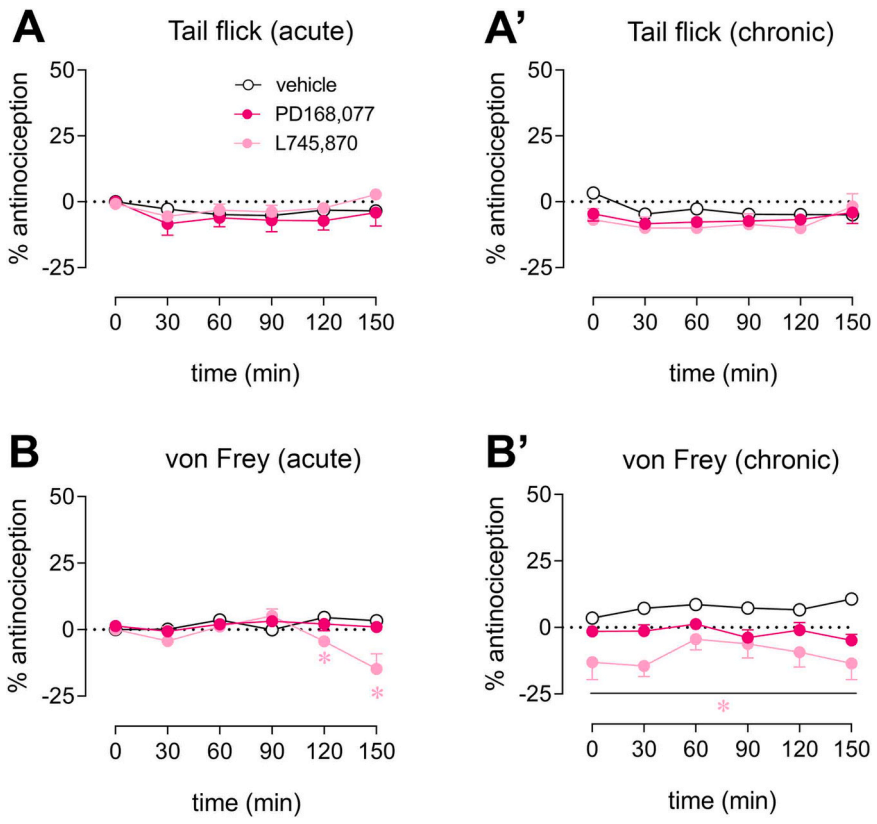

Fig. 1. Evaluation of D_4R stimulation and blockade in thermal and mechanical nociception. Time course of percentage of nociceptive responses following acute (A, B) and chronic (8-day) (A'-B') administration of the D_4R agonist PD168,077 or the D_4R antagonist L745,870 in tail flick (A-A') and von Frey (B-B') test. Neither acute nor chronic PD168,077 elicited antinociceptive effects, whereas chronic D_4R blockade induced mechanical sensitization. Data are expressed as mean ± SEM (n = 8–9 per group). Statistical significance was determined by two-way repeated measures ANOVA followed by Bonferroni's *post hoc* test; $^*p < 0.05$ vs. vehicle.

significantly lower density in lamina I compared to lamina II (lamina I, 88.7% ± 2.8; lamina II, 111.3% ± 2.8; $p < 0.001$, Student's t test; data represent mean OD values ± SEM expressed as percentage of the whole superficial dorsal horn) (Fig. 4D), we performed a lamina-specific analysis to assess potential microscale changes. Consistent with the mRNA data, chronic treatment with morphine and/or PD168,077 did not significantly alter MOR IR (Fig. 4D).

Given that spinal D2-like receptors are involved in dopamine-mediated modulation of pain[26] and have been shown to be upregulated by chronic morphine,[27] we then measured mRNA levels for *Drd2* (D_2R, dopamine D_2 receptor) and *Drd4* (D_4R). No significant changes in *Drd2* or *Drd4* transcript levels were observed following any chronic drug treatment (Fig. 4E, **F**).

D_4R activation alters neurochemical markers associated with non-peptidergic IB4+ C fibers and catecholaminergic projections within the dorsal horn

Chronic opioid administration induces maladaptive plasticity in primary afferent nociceptors projecting to the dorsal horn, affecting both peptidergic and non-peptidergic C fibers,[28,29] thereby contributing to tolerance and opioid-induced sensitization. To address whether D_4R activation could affect these processes, we analyzed changes in the neurochemical markers CGRP, SP, and IB4 within the superficial dorsal horn.

As previously described, CGRP IR (Fig. 5A) and SP IR (Fig. 5B) were predominantly localized to laminae I and the outer part of lamina II (IIo), whereas IB4 binding (Fig. 5C) was enriched in the inner part of lamina II (IIi).[30] Chronic morphine treatment administered either alone or in combination with PD168,077, did not significantly alter CGRP IR in the dorsal horn (Fig. 5A). In contrast, both chronic morphine and morphine combined with PD168,077 significantly increased SP IR within the neuropil (~20% and ~25% increase vs. vehicle, respectively; Fig. 5B). Regarding non-peptidergic C fibers afferents, chronic treatment with PD168,077 alone led to a ~40% increase in IB4 binding, with a similar effect (~48% increase) observed under co-administration with morphine (Fig. 5C).

Considering the critical role of the catecholaminergic system, including descending projections from supraspinal regions and fibers from primary nociceptors in modulating nociceptive processing within the dorsal horn,[11] we next investigated whether chronic morphine treatment and/or concomitant D_4R stimulation might induce adaptive changes in this system. To this end, we analyzed catecholaminergic fibers in laminae I-II, focusing on TH expression and the morphological features of axonal varicosities, which are widely recognized as a reliable indicator of functional neuronal activity. Mirroring the previously observed increase in IB4 binding, a slight but significant increase in TH IR was observed following chronic treatment with PD168,077 alone (~10%) and with combined morphine + PD168,077 (~17%) (Fig. 5D). However, morphological analysis revealed no significant changes in the average size (Fig. 5E) and circularity (Fig. 5F) of TH IR axonal varicosities across treatment groups.

These findings collectively indicate that D_4R activation is associated with changes in neurochemical markers of specific primary afferent populations, particularly non-peptidergic IB4+ C fibers, as well as catecholaminergic projections in the superficial dorsal horn, potentially influencing nociceptive processing during chronic morphine exposure.

D_4R activation counteracts morphine-induced downregulation of vGluT2 but upregulates vGAT in the superficial dorsal horn

The balance between glutamatergic excitation and GABAergic/

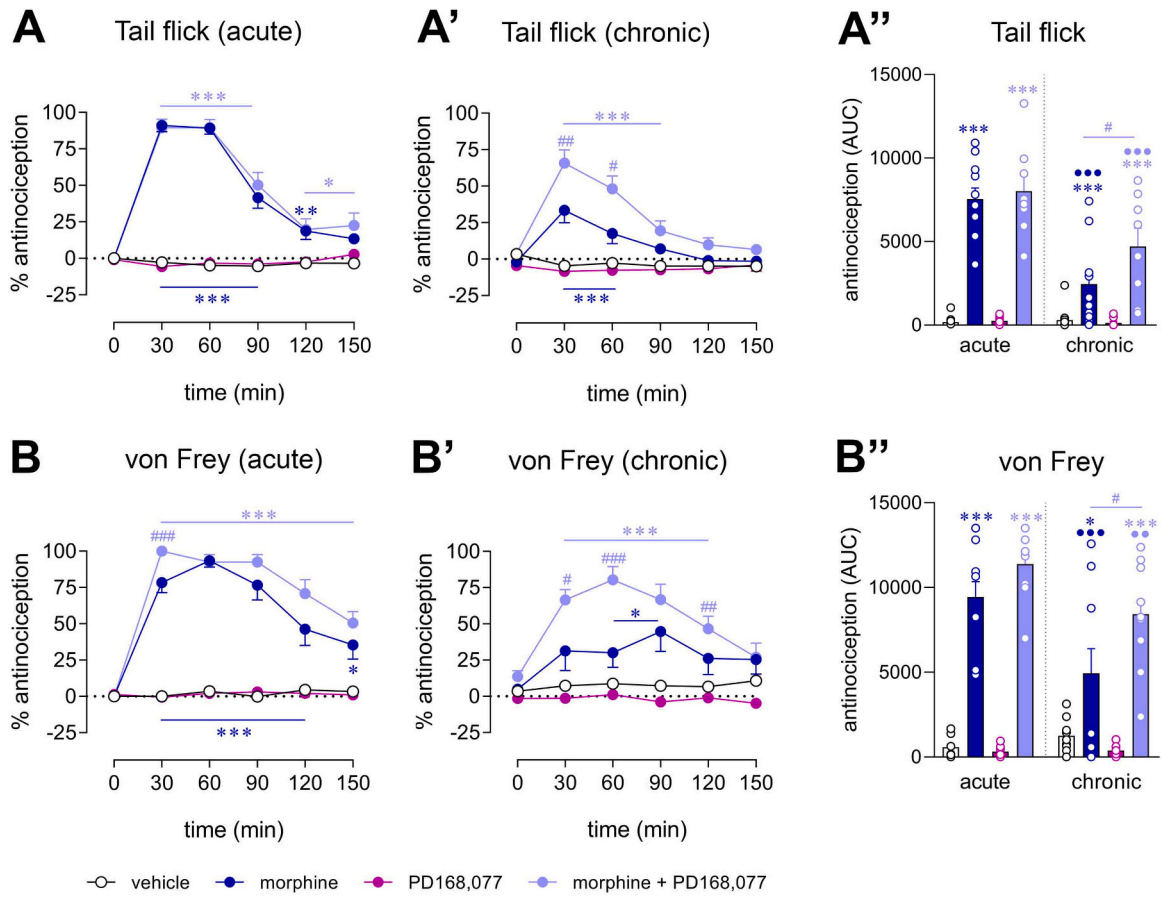

Fig. 2. D_4R activation attenuates morphine-induced antinociceptive tolerance. (A-B') Time-course of percentage of antinociceptive responses during acute (A, B) and 8-day chronic (A', B') morphine administration, either alone or in combination with the D_4R agonist PD168,077, as evaluated by the tail flick (A-A') and von Frey (B-B') tests. Acute PD168,077 administration had no significant effect on morphine-induced analgesia. However, co-administration of PD168,077 during chronic morphine treatment significantly attenuated the development of antinociceptive tolerance. (A'', B'') Global antinociceptive effects for acute and chronic treatments, expressed as the area under the curve (AUC) in the tail flick (A'') and von Frey (B'') tests. Data are expressed as mean ± SEM (n = 8–12 per group). Statistical significance was determined by two-way repeated measures ANOVA followed by Bonferroni's *post-hoc* test $^*p < 0.05$, $^{**}p < 0.01$, $^{***}p < 0.001$ vs. vehicle; $\#p < 0.05$, $\#\#p < 0.01$, $\#\#\#p < 0.001$ vs. morphine; ••p < 0.01, •••p < 0.001 chronic vs. acute treatment.

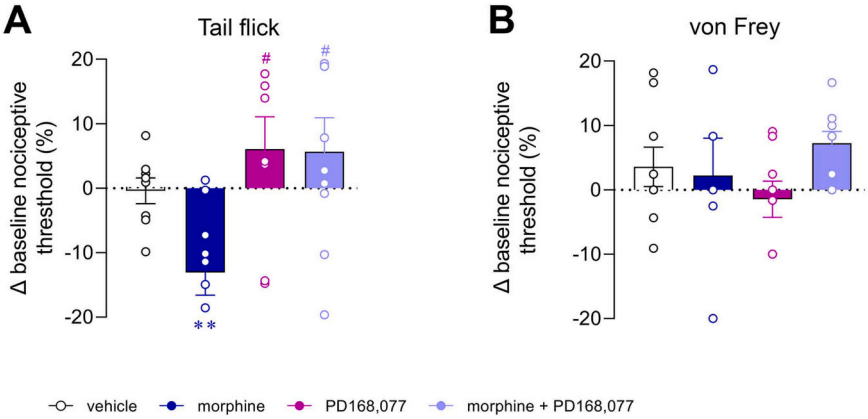

Fig. 3. D_4R activation prevents the development of morphine-induced thermal hyperalgesia. (A) Thermal hyperalgesia and (B) mechanical allodynia were determined as the percentage change in baseline nociceptive thresholds (Δ = day 8 - day 1), assessed by the tail flick and von Frey tests. Chronic morphine administration reduces baseline thermal nociceptive threshold, which was completely reversed by co-administration of PD168,077. Data are expressed as mean ± SEM (n = 8–12 per group). Statistical analyses were performed using one-way ANOVA followed by Bonferroni's *post-hoc* test or Kruskal-Wallis test followed by Dunn's method. $^{**}p < 0.01$ vs. vehicle; $\#p < 0.05$ vs. morphine.

glycinergic inhibition in the dorsal horn determines nociceptive processing and transmission.[5] Dysregulated neurotransmitter release, particularly of glutamate, has been implicated in the development of morphine tolerance.[1] We therefore measured overall neurotransmitter levels in dorsal horn homogenates to evaluate whether D_4R-mediated attenuation of morphine-induced tolerance correlated with changes in

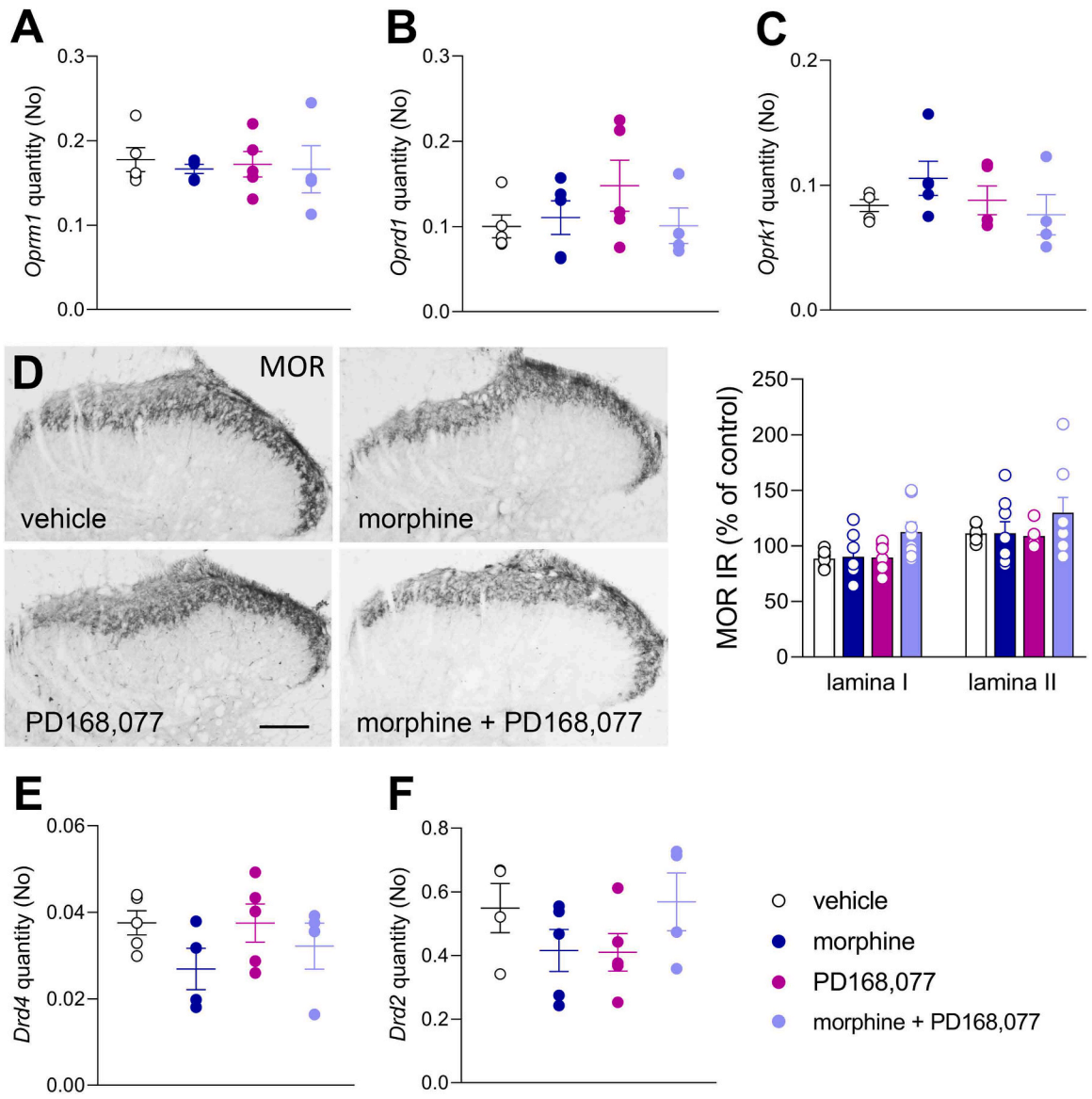

Fig. 4. Chronic D_4R agonist and morphine treatment do not alter opioid or D2-like receptor expression in the dorsal horn. (A-C) mRNA expression levels of the opioid receptor genes *Oprm1* (MOR; A), *Oprd1* (DOR; B) and *Oprk1* (KOR; C) expressed as the mean ± SEM (n = 5 per treatment), calculated from initial mRNA quantity (N0) and normalized to the average of both reference genes, *Tbp* and *Eef1e,* expression levels. (D) Representative photomicrographs showing MOR IR in the superficial dorsal horn after 8 days of chronic morphine and/or PD168,077 treatment on. Scale bar is 125 μm. The semi-quantitative analysis of MOR IR within laminae I and II is presented in the adjacent bar graph. Data are expressed as mean ± SEM (n = 7–8 per group) and normalized as a percentage of vehicle-treated control across the superficial dorsal horn; laminae were analyzed separately. (E-F) mRNA expression of the dopamine receptor genes *Drd4* (D_4R; E) and *Drd2* (D_2R; F) expressed as the mean ± SEM (n = 4–5 per group), calculated from initial mRNA quantity (N0) and normalized to the average of both reference genes expression, *Tbp* and *Eef1e*. All statistical analyses were performed with one-way ANOVA followed by Bonferroniś *post-hoc* test. *Abbreviations:* D_2R, dopamine D_2 receptor; D_4R, dopamine D_4 receptor; DOR, delta opioid receptor; IR, immunoreactivity; KOR, kappa opioid receptor; MOR, mu opioid receptor.

glutamate, GABA, or glycine signaling. Chronic administration of morphine, PD168,077, or their combination did not significantly alter total tissue concentrations of glutamate (Fig. 6A), GABA (Fig. 6B), or glycine (Fig. 6C) relative to vehicle controls.

Despite the absence of detectable changes in the levels of these neurotransmitters in the HPLC experiments, we hypothesized that alterations might occur at the microscale level and/or within specific laminae of the dorsal horn. To test this hypothesis, we assessed vGluT2 and vGAT IR density in laminae I-II of the dorsal horn, given their roles in loading of glutamate and GABA/glycine into presynaptic vesicles at excitatory and inhibitory terminals, respectively.[31–34] A widespread punctate labeling for vGluT2 IR (Fig. 6D) and vGAT IR (Fig. 6E) was observed throughout the spinal cord neuropil. Both markers were more highly expressed in lamina I compared to lamina II (vGluT2: lamina I, 118.5% ± 1.0; lamina II, 82.4% ± 2.3; $p < 0.001$, Student's t test; vGAT: lamina I, 115.0% ± 1.9; lamina II, 85.0 ± 1.9; $p < 0.01$, Student's t test; data represent mean OD values ± SEM expressed as percentage of total IR in the superficial dorsal horn).

As shown in Fig. 6D, an 8-day chronic morphine treatment induced a significant decrease in vGluT2 IR in both lamina I (~25%) and lamina II (~20%), which was completely counteracted by co-administration with PD168,077. In contrast, vGAT IR remained unchanged following chronic morphine alone but exhibited a significant increase in animals receiving both morphine and PD168,077 (lamina I: ~88%; lamina II: ~78%) (Fig. 6E). Chronic PD168,077 alone produced a modest but significant decrease in vGluT2 in lamina I (~13%), whereas no significant changes were observed in lamina II or in vGAT IR in either lamina relative to vehicle controls.

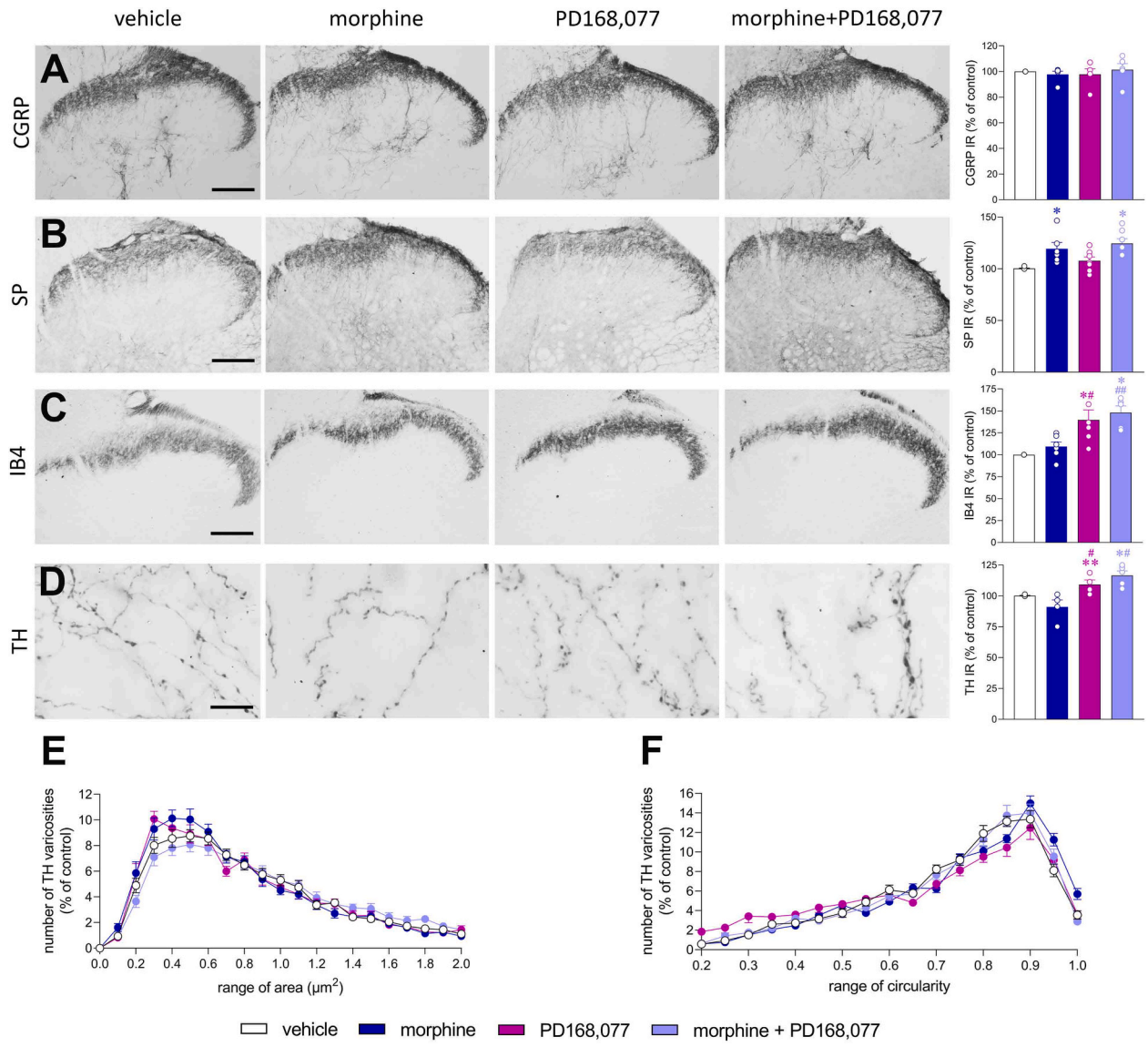

Fig. 5. Chronic D_4R activation induces adaptive changes in non-peptidergic IB4+ C fibers and catecholamine projections in the dorsal horn. (A-D) Representative photomicrographs and corresponding semi-quantitave optical density analysis for CGRP IR(A), SP IR (B), IB4 binding (C) and TH IR (D) in the superficial dorsal horn after 8-day chronic treatment with morphine and/or PD168,077. Data are expressed as mean ± SEM (n = 5–7 per group) and normalized as a percentage of the vehicle-treated control. Statistical significance was determined with the Kruskal-Wallis test followed by Dunn's method, $*p < 0.05$, $**p < 0.01$ vs. vehicle; $\#p < 0.05$, $\#\#p < 0.01$ vs. morphine. Scale bar in A-C is 150 μm and 10 μm in D. (E-F) Morphometric analysis of TH IR varicosities in laminae I-II, showing the frequency distribution (as percentage of total varicosities) categorized by area (μm^2) (E) and circularity (F) following the same chronic treatment regimens. Data are expressed as mean ± SEM (n = 5–7 per group). Statistical analyses were performed using one-way ANOVA followed by Bonferroníś *post-hoc* test or Kruskal-Wallis test followed by Dunn's method. *Abbreviations:* CGRP, calcitonin gene-related peptide; IB4, isolectin B4; IR, immunoreactivity; SP, substance P; TH: tyrosine hydroxylase.

Thus, despite apparently stable global neurotransmitter levels, D_4R activation appears to be associated with changes in the expression of vesicular transporters involved in glutamate and GABA/glycine loading, suggesting a shift toward a more inhibitory microenvironment in the superficial dorsal horn.

D_4R activation during chronic morphine treatment reduces NK1 receptor expression and CREB-dependent activation in lamina I projection neurons

Given that chronic morphine increases P-CREB expression in the dorsal horn, a key driver of opioid tolerance,[35] we hypothesized that D_4R-mediated attenuation of morphine tolerance might involve regulation of this transcription factor. Supporting this hypothesis, D_4R activation not only counteracted the morphine-induced rise in P-CREB (~39%) but also reduced its expression below control levels (~40%) (Fig. 7A).

Together with the marked upregulation of vGAT, these results prompted us to ask which second-order dorsal horn neurons might mediate D_4R-driven shift toward inhibition. In light of the remarkable complexity and still incomplete characterization of spinal dorsal horn circuits,[36] we approached this question as a proof of concept by examining potential changes in the expression of calcium-binding proteins in spinal interneurons, as calcium homeostasis critically shapes the intrinsic spinal circuitry involved in pain processing.[37] Accordingly, we quantified the number of CB, CR and PV interneurons in the superficial dorsal horn and assessed protein expression at the single-cell level. As shown in Supplementary Figure S3A-C, A'-C', neither chronic morphine nor PD168,077 treatment altered the IR of these calcium-binding proteins. However, significant changes in interneuron numbers were observed in some cases (Supplementary Figure 3A''-C''). Specifically,

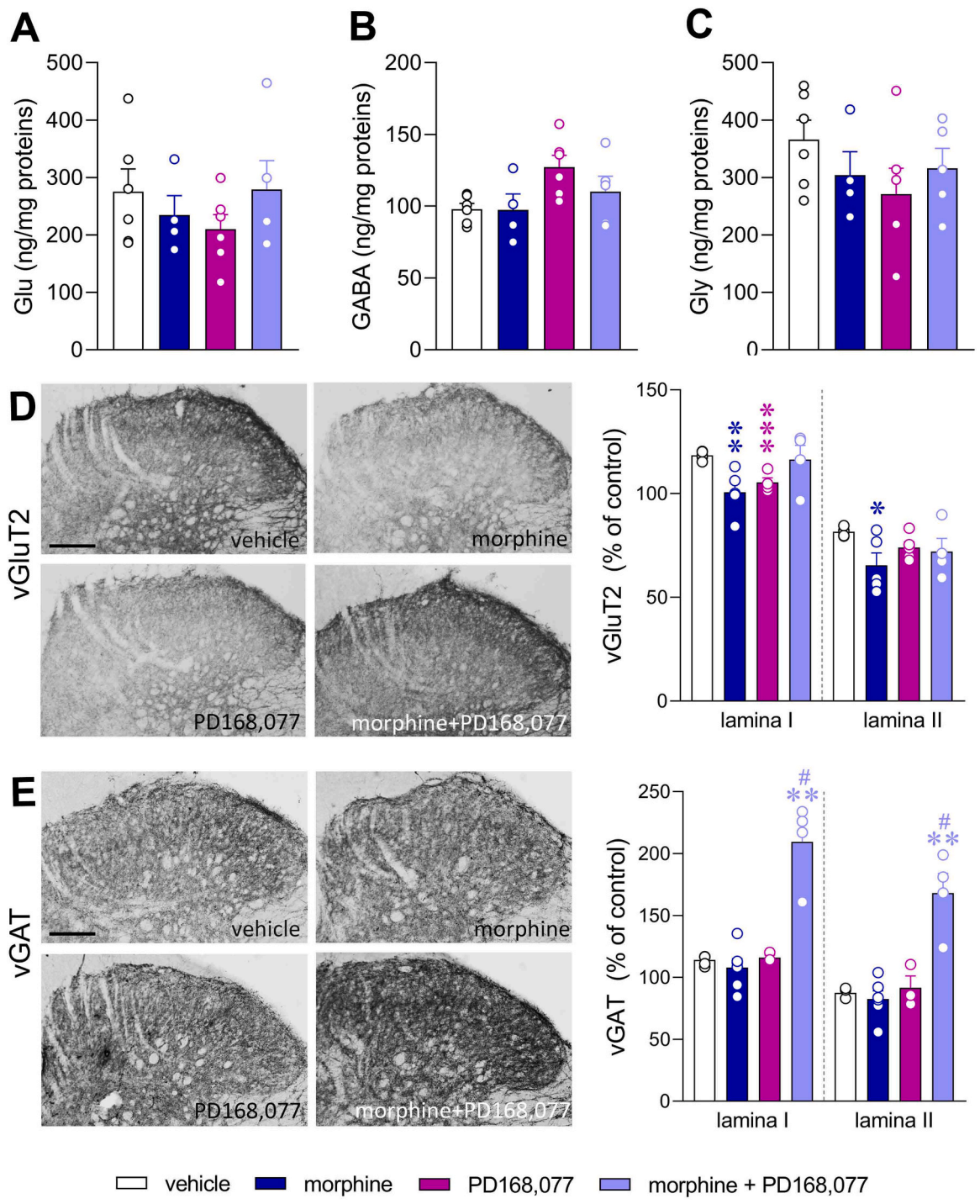

Fig. 6. Chronic D_4R agonist and morphine co-administration upregulate vGAT expression in the superficial dorsal horn. (A-C) Tissue concentrations (ng/mg protein) of glutamate (A), GABA (B) and glycine (C) measured by HPLC after 8 days of daily morphine and/or PD168,077 treatment. No significant differences were observed among treatment groups. Data represent mean ± SEM (n = 5 per group) and were analyzed by one-way ANOVA. (D-E) Representative photomicrographs and corresponding semi-quantitative optical density analysis of vGluT2 IR (D) and vGAT IR (E) in the superficial dorsal horn (laminae I-II) from the same treatment groups. Data represent mean ± SEM (n = 5 per group), normalized as a percentage of the vehicle-treated control and analyzed separately for each lamina, allowing comparisons between them. Statistical analyses were performed with the Kruskal-Wallis test followed by Dunn's method or one-way ANOVA followed by Bonferroni's *post-hoc* test. *$p < 0.05$, **$p < 0.01$, ***$p < 0.001$ vs. vehicle; #$p < 0.05$ vs. morphine. Scale bars are 150 μm. *Abbreviations:* IR, immunoreactivity; vGAT, vesicular GABA transporter; vGluT2, vesicular glutamate transporter isoform 2.

chronic PD168,077 treatment decreased the number of CR interneurons ~25% (Supplementary Figure S3B''), whereas both morphine and morphine + PD168,077 treatments increased the number of PV interneurons ~85% (Supplementary Figure S3C''). The number of CB interneurons was unaffected by any treatment (Supplementary Figure S3A'').

We next evaluated whether these interneurons engage CREB-dependent signaling by analyzing P-CREB co-expression. We found that ~50% of CB (Fig. 7B) and CR (Fig. 7C) interneurons were P-CREB+ in controls, and this proportion remained unchanged following chronic

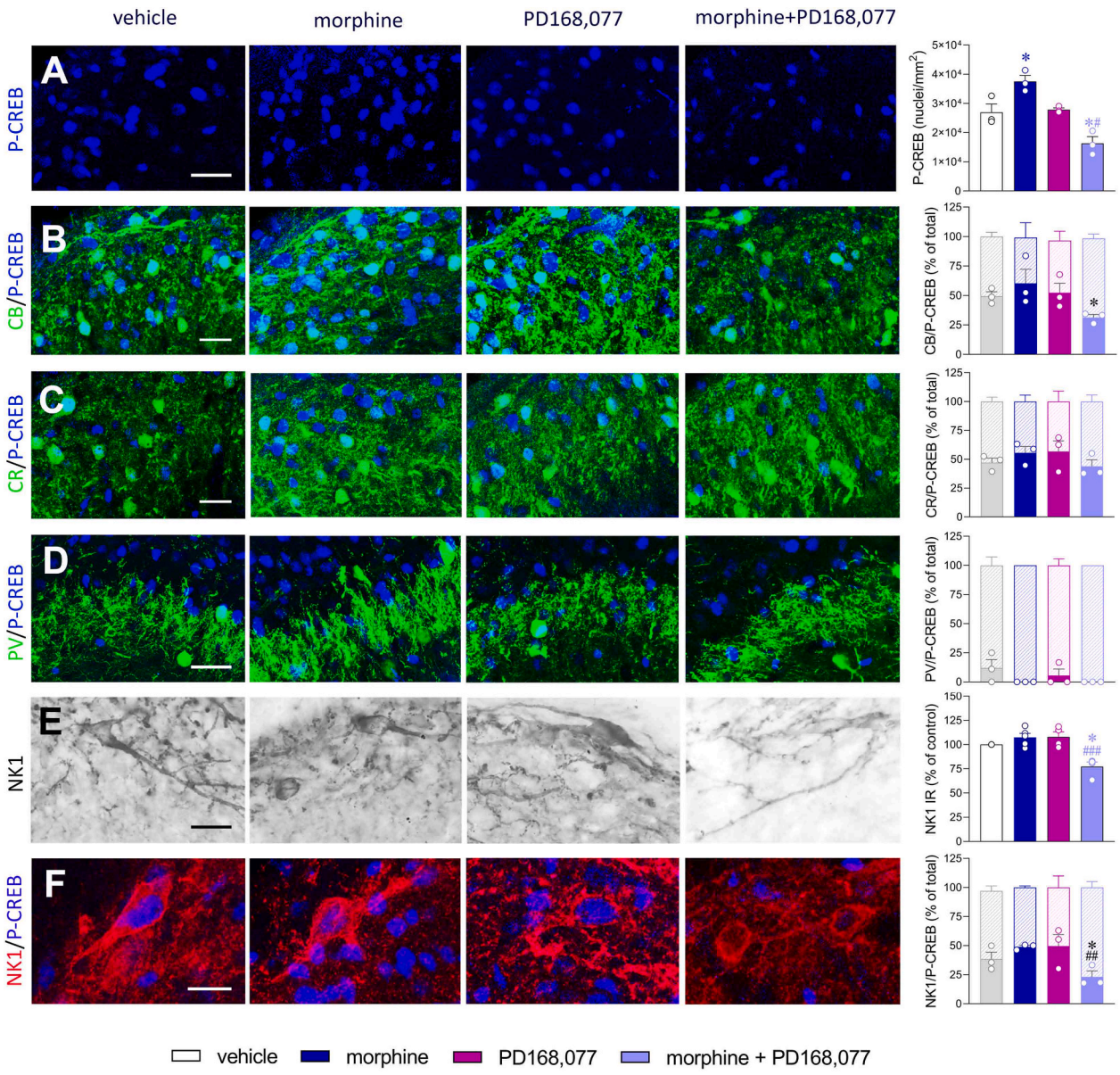

Fig. 7. Chronic D_4R agonist and morphine co-administration downregulates NK1 receptor expression and P-CREB activation in lamina I projection neurons. (A) P-CREB IR in the superficial dorsal horn and corresponding quantitative analysis of 8 days of chronic morphine and/or PD168, 077 treatment. The graph depicts the density of P-CREB+ nuclei (nuclei/mm^2). Data represent mean ± SEM (n = 3 per group) and are expressed as a percentage of the vehicle-treated control. (B-D) Dual-labeled immunofluorescence for P-CREB (blue) and calcium-binding proteins (green): CB (B), CR (C), and PV (D). Histograms show total density of each interneuron subtype, with internal solid bars denoting the percentage of P-CREB co-expression. Data represent mean ± SEM (n = 3 per group). (E) NK1 IR in lamina I projection neurons and semi-quantitative optical density analysis. Data represent mean ± SEM (n = 5 per group) and are expressed as a percentage of the vehicle-treated control. (F) Dual-labeling of P-CREB (blue) and NK1 (red) in lamina I projection neurons. The histogram illustrates the percentage of NK1+ projection neurons, with internal solid bars representing the P-CREB positive subpopulation. Data represent mean ± SEM (n = 3 per group). Statistical analyses were performed with the Kruskal-Wallis test followed by Dunn's method or one-way ANOVA followed by Bonferroníś *post-hoc* test. *$p < 0.05$, vs. vehicle; #$p < 0.05$ vs. morphine. Scale bars are 20 μm. *Abbreviations:* CB, calbindin; CR, calretinin; IR, immunoreactivity; NK1, neurokinin-1 receptor; P-CREB, phosphorylated cAMP response element-binding protein; PV, parvalbumin.

morphine or PD168,077 treatment. Interestingly, combined morphine + PD168,077 selectively reduced the proportion of CB interneurons colocalized with P-CREB (~30%) (Fig. 7B), whereas CR interneurons were unaffected (Fig. 7C). In contrast, PV interneurons rarely exhibited P-CREB expression across all treatment groups (Fig. 7D).

Lastly, we investigated the impact of D_4R activation during chronic (8-day) morphine treatment on lamina I NK1+ projection neurons, which constitute the main output of dorsal horn nociceptive circuitry.[5] We assessed NK1 IR, given that its availability and trafficking critically regulate neuronal excitability,[38] and examined P-CREB expression within these same neurons to determine their activation state. Chronic 8-day treatment with either morphine or PD168,077 alone did not significantly alter NK1 IR (Fig. 7E) or the proportion of NK1+ projection neurons expressing P-CREB (Fig. 7F). Strikingly, combined chronic treatment with morphine and PD168,077 produced a concurrent downregulation of NK1 IR (~23%; Fig. 7E) and reduced the fraction of NK1+ projection neurons positive for P-CREB from ~50% to ~20% (Fig. 7F).

Together, these results suggest that D_4R activation may attenuate morphine-induced tolerance by reducing NK1 receptor expression and CREB-dependent signaling in lamina I projection neurons, thereby potentially contributing to reduced nociceptive output to supraspinal

targets.

Discussion

The progressive decline in opioid analgesic efficacy, together with the emergence of adverse effects such as tolerance, OIH, and addiction, strongly limits the long-term clinical use of opioids.[25] While the precise mechanisms remain elusive, accumulating evidence indicates a functional divergence between the neural substrates mediating opioid analgesia and those driving maladaptive neuroplasticity and adverse effects.[1] Thus, identifying the molecular and cellular components that differentially regulate these processes is essential for developing safer therapeutic strategies. Within this framework, the present study investigated the role of D_4R in modulating morphine analgesia and its potential to mitigate adverse effects associated with chronic morphine exposure.

Our previous work identified the D_4R as a negative modulator of morphine-induced molecular and cellular neuroadaptations within striatal circuits, preventing the development and consolidation of addiction.[15,16,18,23] Here, we extended these findings by showing that concomitant administration of the D_4R agonist PD168,077 with morphine preserves analgesia, markedly attenuates analgesic tolerance, and completely prevents OIH. Furthermore, pharmacological blockade with the selective antagonist L745,870 induced mechanical hypersensitivity, suggesting that endogenous D_4R signaling is required to maintain normal mechanical thresholds.

D_4R modulation of descending catecholaminergic control

Noradrenaline and serotonin are well-established modulators of pain via descending projections arising from the locus coeruleus and raphe nuclei, respectively. In contrast, dopaminergic control has received less attention despite compelling evidence of its functional relevance.[39] This is particularly evident in Parkinson's disease, where degeneration of dopaminergic pathways alters both pain perception and nociceptive processing.[40]

Dopaminergic innervation of the spinal cord primarily originates from hypothalamic A11 neurons[41] and inhibits responses to noxious and innocuous stimuli by reducing dorsal horn excitability via D2-like receptors.[14] Our results expand on this framework by showing that D_4R activation increases spinal TH IR, suggesting enhanced catecholamine tone. Since D_4R expression is absent in A11 and locus coeruleus neurons,[42] this effect likely arises via D_4R-expressing neurons in the cingulate and prefrontal cortices,[43] which innervate A11[44] and locus coeruleus,[45] respectively. A discrete subpopulation of catecholaminergic neurons also exists in the dorsal root ganglia,[46–48] which may provide an additional peripheral site for D_4R-mediated modulation of sensory signaling.

Dopamine receptors are widely expressed in pain circuits.[12,49] It has been described that D2-like receptors mediate antinociception and engage in functional crosstalk with opioid receptors, thereby modulating opioid-induced analgesia and tolerance.[14,50–52] However, the relative contribution of the different D2-like receptors subtypes—D_2R, D_3R, and D_4R—remains controversial due to their distinct actions[49] and the lack of selective pharmacological tools. Anatomical [19] and functional[20,50,53] evidence indicates that D_4R is expressed at both pre- and postsynaptic sites in the spinal cord, supporting a role in modulation of both primary afferent nociceptors and second-order dorsal horn neurons. Nevertheless, neither previous studies nor our PCR-based analysis has resolved its precise subcellular localization, which remains an important issue for future high-resolution studies.

D_4R drives structural remodeling of non-peptidergic C afferents

A key finding of this study is the selective alteration of markers associated with non-peptidergic C fibers, while peptidergic subtypes remained unchanged. Long-term D_4R activation increased IB4 binding in presynaptic terminals, even under chronic morphine. This aligns with previous studies showing that D_4R activation reduces high–voltage-gated Ca^{2+} currents in these fibers via Cav2.2 Ca^{2+} channels, limiting neurotransmitter release.[53] D_4R also mediates dopamine-induced inhibition of excitatory transmission from Aδ- and C nociceptors onto lamina I projection neurons.[20]

To define the structural basis for this modulation, we propose that the enhanced IB4 binding may reflect a remodeling of presynaptic microarchitecture. IB4 recognizes molecules bearing terminal α-D-galactose, including globoside-type glycosphingolipids,[54] with iGb3 representing a likely target,[55] and cytoskeletal components such as light and medium neurofilament subunits.[56] Globosides are key components of lipid rafts and contribute to the organization of higher-order clustering of raft-associated proteins.[57] Accordingly, D_4R-mediated changes in these molecules could alter raft architecture and downstream signaling.[58] This concept is exemplified by diseases like Fabry disease, where altered Gb3/iGb3 homeostasis disrupt lipid raft organization and impairs nociceptor function.[59] Likewise, changes in neurofilament composition or organization can influence presynaptic terminal structure and stability, thereby affecting neurotransmitter release.[60] In summary, these observations suggest that D_4R is associated with structural changes in non-peptidergic C fibers, potentially involving the reorganization of membrane microdomains and the cytoskeletal architecture of presynaptic terminals, a mechanism that warrants further high-resolution investigation.

D_4R promotes an inhibitory state in dorsal horn circuitry and reduces NK1+ projection neuron excitability

Nociceptive signaling within the spinal dorsal horn is defined by the dynamic interplay between glutamatergic excitation, originating from primary afferents and spinal second-order neurons, and GABAergic/glycinergic inhibition, mediated primarily by local interneurons.[5] Hyperexcitability, due to increased glutamate[61,62] or reduced inhibition,[63,64] underlies opioid-induced tolerance and sensitization.

Vesicular neurotransmitter transporters (vGluTs and vGAT) serve as pivotal regulatory points in this balance, determining synaptic efficacy by controlling the loading of glutamate and GABA/glycine into presynaptic vesicles, respectively.[65,66] vGluT2 has been critically implicated in maladaptive opioid-induced plasticity, with its upregulation consistently reported in paradigms associated with a complete loss of analgesia.[67] In contrast, our results show a significant downregulation of vGluT2 in the superficial dorsal horn following chronic morphine administration. This reduction likely represents a compensatory attempt to limit presynaptic excitatory drive, consistent with our observation that analgesia is not yet fully abolished. However, the simultaneous emergence of hyperalgesia indicates that this compensatory vGluT2 reduction is insufficient to prevent sensitization, likely to other converging maladaptive processes, such as increased SP expression (own result)[68] and enhanced NMDA receptor function.[69]

Strikingly, D_4R agonism not only prevented the morphine-induced reduction in vGluT2 expression but also promoted a robust upregulation of vGAT. This dual action on the vesicular machinery (i.e., maintaining excitatory homeostasis while dramatically enhancing inhibitory potential) strongly suggests that D_4R activation shifts dorsal horn circuitry toward a predominantly inhibitory state. A central feature of this regulation is the broad suppression of P-CREB signaling, a well-established marker of spinal sensitization and tolerance.[35] While chronic morphine pathologically induces P-CREB, D_4R activation suppressed this response to levels below baseline. Importantly, this molecular inhibition correlates with the behavioral preservation of analgesia and prevention of opioid-induced hyperalgesia. By mapping P-CREB modulation across distinct spinal neuronal populations, we identified two converging postsynaptic mechanisms through which D_4R may impose an inhibitory bias on dorsal horn circuitry.

First, in CB interneurons, critical mediators of nociceptive transmission,[70] the reduction of CREB-dependent transcription likely constrain pro-nociceptive relay activity. Second, in lamina I NK1+ projection neurons, the maintenance of P-CREB expression in morphine-tolerant animals at levels comparable to control indicates sustained transmission to supraspinal targets. Given that NK1 upregulation and SP release are hallmarks of hyperalgesia,[9] these active NK1+ projection neurons likely sustain the nociceptive drive to higher centers, thereby contributing to tolerance. Notably, D_4R-mediated downregulation of NK1 receptors mirrors the functional effect of the selective ablation of neurons in preventing opioid-induced hyperalgesia and tolerance,[6,8] effectively silencing spinal pain-output gateway. Mechanistically, this downregulation is likely mediated by the presence of a functional CRE binding site in the *Tacr1* (NK1 receptor) promoter.[71] Consequently, the suppression of P-CREB within these projections neurons provides a molecular link between D_4R signaling and the decreased excitability of lamina I output neurons.[72,73]

Despite these findings, some limitations should be considered. Experiments were conducted exclusively in male rats to maintain consistency with prior work, and it remains to be determined whether the effects of D_4R activation extend to females, given well-established sex differences in pain processing and opioid responses. In addition, the present study relies primarily on neurochemical and anatomical measures and does not directly assess neuronal activity. Future studies incorporating both sexes and functional approaches, such as calcium imaging, electrophysiological recording, or assays of neurotransmitter release in spinal cord slices or cultured DRG neurons, will be required to further define de underlying mechanisms.

In summary, our findings position D_4R as a central integrator of spinal nociceptive control during chronic morphine exposure. Through presynaptic regulation of sensory inputs and postsynaptic enforcement of an inhibitory state, D_4R activation rebalances excitatory-inhibitory signaling. Notably, these postsynaptic effects emerge selectively under opioid challenge, pointing to a state-dependent cross-talk with opioid receptors that limits maladaptive, but not analgesic, signaling. Together, this dual and conditional mode of action identifies D_4R as a strategically positioned modulatory target to preserve opioid analgesia while restraining its long-term liabilities.

CRediT authorship contribution statement

MPV: conceptualization; data curation; formal analysis; investigation; methodology; writing original draft; writing-review and editing. MAR: conceptualization; supervision; writing-review and editing. ARV: formal analysis; funding acquisition; methodology. BG: funding acquisition; writing-review and editing. IFJ: methodology. MMR: methodology. IAB: methodology. CR: funding acquisition; writing-review and editing. AR: conceptualization; formal analysis; investigation; supervision; writing original draft; writing-review and editing.

Study pre-registration statement/Patient and public involvement

This study was not pre-registered. No patients or members of the public were involved.

Declaration of Generative AI and AI-assisted technologies in the writing process

Artificial intelligence-baes tools were used to improve grammar, clarity, and readability of the manuscript. All analysis, interpretations, and conclusions were performed by the authors.

Funding

This research was funded by: Spanish Ministry of Science, Innovation and Universities (MICIU) (PID2023–148753OB-I00); Junta de Andalucía (Spain) (P09-CVI-4702 and PPRO-CTS161-G-2023); ARV was supported by the Ministerio de Ciencia e Innovación (MICIU) / Agencia Estatal de Investigación (AEI) and the European Social Fund Plus (RYC2021–034611-I).

Acknowledgments

The authors thank the Central Research Support Services of the University of Málaga (Proteomics, Molecular Biology, and Microscopy units) for their technical support. The authors also acknowledge the Animal Experimentation and Behavior Center (CECA) of the University of Málaga for animal care and support with experimental procedure. Open access funding was provided by the Universidad de Málaga / CBUA.

Appendix A. Supporting information

Supplementary data associated with this article can be found in the online version at doi:10.1016/j.jpain.2026.106308.

Data availability

The data that support the findings of this study are available from the corresponding author upon reasonable request.

References

1. Roeckel LA, Le Coz GM, Gavériaux-Ruff C, Simonin F. Opioid-induced hyperalgesia: cellular and molecular mechanisms. *Neuroscience*. 2016;338:160–182. https://doi.org/10.1016/j.neuroscience.2016.06.029.
2. Chu LF, Angst MS, Clark D. Opioid-induced hyperalgesia in humans: molecular mechanisms and clinical considerations. *Clin J Pain*. 2008;24(6):479–496. https://doi.org/10.1097/AJP.0b013e31816b2f43.
3. Huang M, Luo L, Wang W, et al. Targeting excitatory glutamate receptors for morphine tolerance: a narrative review. *CNS Neurosci Ther*. 2025;31(6). https://doi.org/10.1111/cns.70468.
4. Johnston IN, Milligan ED, Wieseler-Frank J, et al. A role for proinflammatory cytokines and fractalkine in analgesia, tolerance, and subsequent pain facilitation induced by chronic intrathecal morphine. *J Neurosci*. 2004;24(33):7353–7365. https://doi.org/10.1523/JNEUROSCI.1850-04.2004.
5. Todd AJ. Neuronal circuitry for pain processing in the dorsal horn. *Nat Rev Neurosci*. 2010;11(12):823–836. https://doi.org/10.1038/nrn2947.
6. Weisshaar CL, Winkelstein BA. Ablating spinal nk1-bearing neurons eliminates the development of pain and reduces spinal neuronal hyperexcitability and inflammation from mechanical joint injury in the rat. *J Pain*. 2014;15(4):378–386. https://doi.org/10.1016/j.jpain.2013.12.003.
7. Khasabov SG, Rogers SD, Ghilardi JR, Peters CM, Mantyh PW, Simone DA. Spinal neurons that possess the substance P receptor are required for the development of central sensitization. *J Neurosci*. 2002;22(20):9086–9098. https://doi.org/10.1523/JNEUROSCI.22-20-09086.2002.
8. Vera-Portocarrero LP, Zhang ET, King T, et al. Spinal NK-1 receptor expressing neurons mediate opioid-induced hyperalgesia and antinociceptive tolerance via activation of descending pathways. *Pain*. 2007;129(1-2):35–45. https://doi.org/10.1016/j.pain.2006.09.033.
9. King T, Gardell LR, Wang R, et al. Role of NK-1 neurotransmission in opioid-induced hyperalgesia. *Pain*. 2005;116(3):276–288. https://doi.org/10.1016/j.pain.2005.04.014.
10. Suzuki R, Morcuende S, Webber M, Hunt SP, Dickenson AH. Superficial NK1-expressing neurons control spinal excitability through activation of descending pathways. *Nat Neurosci*. 2002;5(12):1319–1326. https://doi.org/10.1038/nn966.
11. Millan MJ. Descending control of pain. *Prog Neurobiol*. 2002;66(6):355–474. https://doi.org/10.1016/S0301-0082(02)00009-6.
12. Puopolo M. The hypothalamic-spinal dopaminergic system: a target for pain modulation. *Neural Regen Res*. 2019;14(6):925–930. https://doi.org/10.4103/1673-5374.250567.
13. Yang HW, Zhou LJ, Hu NW, Xin WJ, Liu XG. Activation of spinal D1/D5 receptors induces late-phase LTP of C-fiber-evoked field potentials in rat spinal dorsal horn. *J Neurophysiol*. 2005;94(2):961–967. https://doi.org/10.1152/jn.01324.2004.
14. Taniguchi W, Nakatsuka T, Miyazaki N, et al. vivo patch-clamp analysis of dopaminergic antinociceptive actions on substantia gelatinosa neurons in the spinal cord. *Pain*. 2011;152(1):95–105. https://doi.org/10.1016/j.pain.2010.09.034.
15. Rivera A, Gago B, Suárez-Boomgaard D, et al. Dopamine D4 receptor stimulation prevents nigrostriatal dopamine pathway activation by morphine: relevance for drug addiction. *Addict Biol*. 2017;22(5):1232–1245. https://doi.org/10.1111/adb.12407.
16. Rivera A, Suárez-Boomgaard D, Miguelez C, et al. Dopamine D4 receptor is a regulator of morphine-induced plasticity in the rat dorsal striatum. *Cells*. 2022;11(1). https://doi.org/10.3390/cells11010031.

17. Valderrama-Carvajal A, Irizar H, Gago B, et al. Transcriptomic integration of D4R and MOR signaling in the rat caudate putamen. *Sci Rep*. 2018;8(1). https://doi.org/10.1038/s41598-018-25604-4.
18. Suárez-Boomgaard D, Gago B, Valderrama-Carvajal A, et al. Dopamine D4 receptor counteracts morphine-induced changes in μ opioid receptor signaling in the striosomes of the rat caudate putamen. *Int J Mol Sci*. 2014;15(1):1481–1498. https://doi.org/10.3390/ijms15011481.
19. Zhu H, Clemens S, Sawchuk M, Hochman S. Expression and distribution of all dopamine receptor subtypes (D1-D5) in the mouse lumbar spinal cord: A real-time polymerase chain reaction and non-autoradiographic in situ hybridization study. *Neuroscience*. 2007;149(4):885–897. https://doi.org/10.1016/j.neuroscience.2007.07.052.
20. Lu Y, Doroshenko M, Lauzadis J, et al. Presynaptic inhibition of primary nociceptive signals to dorsal horn lamina I neurons by dopamine. *J Neurosci*. 2018;38(41):8809–8821. https://doi.org/10.1523/JNEUROSCI.0323-18.2018.
21. Gago B, Fuxe K, Agnati L, Peñafiel A, De La Calle A, Rivera A. Dopamine D4 receptor activation decreases the expression of μ-opioid receptors in the rat striatum. *J Comp Neurol*. 2007;502(3):358–366. https://doi.org/10.1002/cne.21327.
22. Deuis JR, Dvorakova LS, Vetter I. Methods Used to Evaluate Pain Behaviors in Rodents. *Front Mol Neurosci*. 2017;10. https://doi.org/10.3389/FNMOL.2017.00284.
23. Negrete-Díaz JV, Shumilov K, Real MÁ, et al. Pharmacological activation of dopamine D4 receptor modulates morphine-induced changes in the expression of GAD65/67 and GABAB receptors in the basal ganglia. *Neuropharmacology*. 2019;152:22–29. https://doi.org/10.1016/j.neuropharm.2019.01.024.
24. Ruiz-Villalba A, Mattiotti A, Gunst Q, Cano-Ballesteros S, Van Den Hoff M, Ruijter JM. Reference genes for gene expression studies in the mouse heart. *Sci Rep*. 2017;7(1):1–9. https://doi.org/10.1038/s41598-017-00043-9.
25. Rivat C, Ballantyne J. The dark side of opioids in pain management: Basic science explains clinical observation. *Pain Rep*. 2016;1(2). https://doi.org/10.1097/PR9.0000000000000570.
26. Tang D liang, Luan Y wen, Zhou C yi, Xiao C. D2 receptor activation relieves pain hypersensitivity by inhibiting superficial dorsal horn neurons in parkinsonian mice. *Acta Pharm Sin*. 2021;42(2):189–198. https://doi.org/10.1038/s41401-020-0433-3.
27. Dai WL, Xiong F, Yan B, et al. Blockade of neuronal dopamine D2 receptor attenuates morphine tolerance in mice spinal cord. *Sci Rep*. 2016;6. https://doi.org/10.1038/srep38746.
28. Khomula EV, Araldi D, Bonet IJM, Levine JD. Opioid-induced hyperalgesic priming in single nociceptors. *J Neurosci*. 2021;41(1):31–46. https://doi.org/10.1523/JNEUROSCI.2160-20.2020.
29. Ossipov MH, Lai J, King T, Vanderah TW, Porreca F. Underlying mechanisms of pronociceptive consequences of prolonged morphine exposure. *Biopolym - Pept Sci Sect*. 2005;80(2-3):319–324. https://doi.org/10.1002/bip.20254.
30. Motzkin JC, Basbaum AI, Crowther AJ. Neuroanatomy of the nociceptive system: From nociceptors to brain networks. *Int Rev Neurobiol*. 2024;179:1–39. https://doi.org/10.1016/bs.irn.2024.10.008.
31. Li JL, Fujiyama F, Kaneko T, Mizuno N. Expression of vesicular glutamate transporters, VGluT1 and VGluT2, in axon terminals of nociceptive primary afferent fibers in the superficial layers of the medullary and spinal dorsal horns of the rat. *J Comp Neurol*. 2003;457(3):236–249. https://doi.org/10.1002/cne.10556.
32. Yamada MH, Nishikawa K, Kubo K, Yanagawa Y, Saito S. Impaired glycinergic synaptic transmission and enhanced inflammatory pain in mice with reduced expression of vesicular GABA transporter (VGAT). *Mol Pharm*. 2012;81(4):610–619. https://doi.org/10.1124/mol.111.076083.
33. Browne TJ, Gradwell MA, Iredale JA, et al. Transgenic Cross-Referencing of Inhibitory and Excitatory Interneuron Populations to Dissect Neuronal Heterogeneity in the Dorsal Horn. *Front Mol Neurosci*. 2020;13. https://doi.org/10.3389/fnmol.2020.00032.
34. Pin JP, Bettler B. Organization and functions of mGlu and GABA B receptor complexes. *Nature*. 2016;540(7631):60–68. https://doi.org/10.1038/nature20566.
35. Takahashi K, Yi H, Gu J, et al. The mitochondrial calcium uniporter contributes to morphine tolerance through pCREB and CPEB1 in rat spinal cord dorsal horn. *Br J Anaesth*. 2019;123(2):e226–e238. https://doi.org/10.1016/j.bja.2019.05.027.
36. Boyle KA, Gutierrez-Mecinas M, Polgár E, et al. A quantitative study of neurochemically defined populations of inhibitory interneurons in the superficial dorsal horn of the mouse spinal cord. *Neuroscience*. 2017;363:120–133. https://doi.org/10.1016/j.neuroscience.2017.08.044.
37. Schwaller B, Meyer M, Schiffmann S. "New" functions for "old" proteins: The role of the calcium-binding proteins calbindin D-28k, calretinin and parvalbumin, in cerebellar physiology. Studies with knockout mice. *Cerebellum*. 2002;1(4):241–258. https://doi.org/10.1080/147342202320883551.
38. Saeed AW, Ribeiro-da-Silva A. De novo expression of neurokinin-1 receptors by spinoparabrachial lamina I pyramidal neurons following a peripheral nerve lesion. *J Comp Neurol*. 2013;521(8):1915–1928. https://doi.org/10.1002/cne.23267.
39. Bravo L, Llorca-Torralba M, Berrocoso E, Micó JA. Monoamines as drug targets in chronic pain: focusing on neuropathic pain. *Front Neurosci*. 2019;13. https://doi.org/10.3389/fnins.2019.01268.
40. Buhmann C, Wrobel N, Grashorn W, et al. Pain in Parkinson disease: a cross-sectional survey of its prevalence, specifics, and therapy. *J Neurol*. 2017;264(4):758–769. https://doi.org/10.1007/s00415-017-8426-y.
41. Koblinger K, Füzesi T, Ejdrygiewicz J, Krajacic A, Bains JS, Whelan PJ. Characterization of A11 neurons projecting to the spinal cord of mice. *PLoS One*. 2014;9(10). https://doi.org/10.1371/journal.pone.0109636.
42. Khan ZU, Gutiérrez A, Martín R, Peñafiel A, Rivera A, De La Calle A. Differential regional and cellular distribution of dopamine D2-like receptors: An immunocytochemical study of subtype-specific antibodies in rat and human brain. *J Comp Neurol*. 1998;402(3):353–371. https://doi.org/10.1002/(SICI)1096-9861(19981221)402:3<353::AID-CNE5>3.0.CO;2-4.
43. Rivera A, Peñafiel A, Megías M, et al. Cellular localization and distribution of dopamine D4 receptors in the rat cerebral cortex and their relationship with the cortical dopaminergic and noradrenergic nerve terminal networks. *Neuroscience*. 2008;155(3):997–1010. https://doi.org/10.1016/j.neuroscience.2008.05.060.
44. Abrahamson EE, Moore RY. The posterior hypothalamic area: Chemoarchitecture and afferent connections. *Brain Res*. 2001;889(1-2):1–22. https://doi.org/10.1016/S0006-8993(00)03015-8.
45. Breton-Provencher V, Drummond GT, Sur M. Locus Coeruleus Norepinephrine in Learned Behavior: Anatomical Modularity and Spatiotemporal Integration in Targets. *Front Neural Circuits*. 2021;15. https://doi.org/10.3389/fncir.2021.638007.
46. Brumovsky P, Villar MJ, Hökfelt T. Tyrosine hydroxylase is expressed in a subpopulation of small dorsal root ganglion neurons in the adult mouse. *Exp Neurol*. 2006;200(1):153–165. https://doi.org/10.1016/j.expneurol.2006.01.023.
47. Brumovsky PR. Dorsal root ganglion neurons and tyrosine hydroxylase - An intriguing association with implications for sensation and pain. *Pain*. 2016;157(2):314–320. https://doi.org/10.1097/j.pain.0000000000000381.
48. Usoskin D, Furlan A, Islam S, et al. Unbiased classification of sensory neuron types by large-scale single-cell RNA sequencing. *Nat Neurosci*. 2015;18(1):145–153. https://doi.org/10.1038/nn.3881.
49. Wang XQ, Mokhtari T, Zeng YX, Yue LP, Hu L. The distinct functions of dopaminergic receptors on pain modulation: a narrative review. *Neural Plast*. 2021;2021, 6682275. https://doi.org/10.1155/2021/6682275.
50. Almanza A, Simón-Arceo K, Coffeen U, et al. A D2-like receptor family agonist produces analgesia in mechanonociception but not in thermonociception at the spinal cord level in rats. *Pharm Biochem Behav*. 2015;137:119–125. https://doi.org/10.1016/j.pbb.2015.08.013.
51. Tamae A, Nakatsuka T, Koga K, et al. Direct inhibition of substantia gelatinosa neurones in the rat spinal cord by activation of dopamine D2-like receptors. *J Physiol*. 2005;568(1):243–253. https://doi.org/10.1113/jphysiol.2005.091843.
52. Alderete J, Tanzillo A, Miller J, et al. Opposing effects of mu opioid receptors on dopamine D1 and D2 receptor expressing neurons in opioid mediated antinociception. *J Pain*. 2025;35, 105474. https://doi.org/10.1016/j.jpain.2025.105474.
53. Segura-Chama P, Luis E, Almanza A, Pellicer F, Hernández-Cruz A, Mercado F. Modulation of intracellular calcium concentration by D2-like DA receptor agonists in non-peptidergic DRG neurons is mediated mainly by D4 receptor activation. *Neurosci Lett*. 2020;736. https://doi.org/10.1016/j.neulet.2020.135267.
54. Jabbarzadeh-Tabrizi S, Boutin M, Day TS, et al. Assessing the role of glycosphingolipids in the phenotype severity of Fabry disease mouse model. *J Lipid Res*. 2020;61(11):1410–1423. https://doi.org/10.1194/jlr.RA120000909.
55. Zhou D, Mattner J, Cantu C, et al. Lysosomal glycosphingolipid recognition by NKT cells. *Science*. 2004;306(5702):1786–1789. https://doi.org/10.1126/science.1103440.
56. Fullmer, Riedl MS, Higgins LA, Elde R. Identification of some lectin IB4 binding proteins in rat dorsal root ganglia. *Neuroreport*. 2004;15(11):1705–1709. https://doi.org/10.1097/01.wnr.0000136037.54095.64.
57. Nutikka A, Lingwood C. Generation of receptor-active, globotriaosyl ceramide/cholesterol lipid "rafts" in vitro: a new assay to define factors affecting glycosphingolipid receptor activity. *Glycoconj J*. 2003;20(1):33–38. https://doi.org/10.1023/B:GLYC.0000016740.69726.fb.
58. Labilloy A, Youker RT, Bruns JR, et al. Altered dynamics of a lipid raft associated protein in a kidney model of Fabry disease. *Mol Genet Metab*. 2014;111(2):184–192. https://doi.org/10.1016/j.ymgme.2013.10.010.
59. Choi L, Vernon J, Kopach O, et al. The Fabry disease-associated lipid lyso-Gb3 enhances voltage-gated calcium currents in sensory neurons and causes pain. *Neurosci Lett*. 2015;594:163–168. https://doi.org/10.1016/j.neulet.2015.01.084.
60. Yuan A, Nixon RA. Specialized roles of neurofilament proteins in synapses: Relevance to neuropsychiatric disorders. *Brain Res Bull*. 2016;126(Pt 3):334–346. https://doi.org/10.1016/j.brainresbull.2016.09.002.
61. Scherrer G, Low SA, Wang X, et al. VGLUT2 expression in primary afferent neurons is essential for normal acute pain and injury-induced heat hypersensitivity. *Proc Natl Acad Sci USA*. 2010;107(51):22296–22301. https://doi.org/10.1073/pnas.1013413108.
62. Wang L, Chen SR, Ma H, Chen H, Hittelman WN, Pan HL. Regulating nociceptive transmission by VGluT2-expressing spinal dorsal horn neurons. *J Neurochem*. 2018;147(4):526–540. https://doi.org/10.1111/jnc.14588.
63. Kearns A, Jayasi J, Liu X, et al. Neuron type-dependent synaptic activity in the spinal dorsal horn of opioid-induced hyperalgesia mouse model. *Front Synaptic Neurosci*. 2021;13, 748929. https://doi.org/10.3389/fnsyn.2021.748929.
64. Koga K, Kanehisa K, Kohro Y, et al. Chemogenetic silencing of GABAergic dorsal horn interneurons induces morphine-resistant spontaneous nocifensive behaviours. *Sci Rep*. 2017;7(1):4739. https://doi.org/10.1038/s41598-017-04972-3.
65. Chaudhry FA, Reimer RJ, Bellocchio EE, et al. The vesicular GABA transporter, VGAT, localizes to synaptic vesicles in sets of glycinergic as well as GABAergic neurons. *J Neurosci*. 1998;18(23):9733–9750. https://doi.org/10.1523/jneurosci.18-23-09733.1998.
66. Herman MA, Ackermann F, Trimbuch T, Rosenmund C. Vesicular glutamate transporter expression level affects synaptic vesicle release probability at hippocampal synapses in culture. *J Neurosci*. 2014;34(35):11781–11791. https://doi.org/10.1523/JNEUROSCI.1444-14.2014.
67. He L, Xu W, Zhang C, et al. Dysregulation of vesicular glutamate transporter VGluT2 via BDNF/TrkB pathway contributes to morphine tolerance in mice. *Front Pharm*. 2022;13, 861786. https://doi.org/10.3389/fphar.2022.861786.

68. Powell KJ, Ma W, Sutak M, Doods H, Quirion R, Jhamandas K. Blockade and reversal of spinal morphine tolerance by peptide and non-peptide calcitonin gene-related peptide receptor antagonists. *Br J Pharm*. 2000;131(5):875–884. https://doi.org/10.1038/sj.bjp.0703655.
69. Chen SR, Chen H, Jin D, Pan HL. Brief opioid exposure paradoxically augments primary afferent input to spinal excitatory neurons via α2δ-1–dependent presynaptic NMDA receptors. *J Neurosci*. 2022;42(50):9315–9329. https://doi.org/10.1523/JNEUROSCI.1704-22.2022.
70. Egea J, Malmierca E, Rosa AO, et al. Participation of calbindin-D28K in nociception: results from calbindin-D 28K knockout mice. *Pflug Arch Eur J Physiol*. 2012;463(3):449–458. https://doi.org/10.1007/s00424-011-1063-x.
71. Hershey AD, Dykema PE, Krause JE. Organization, structure, and expression of the gene encoding the rat substance P receptor. *J Biol Chem*. 1991;266(7):4366–4374. https://doi.org/10.1016/s0021-9258(20)64331-9.
72. Anderson LE, Seybold VS. Phosphorylated cAMP response element binding protein increases in neurokinin-1 receptor-immunoreactive neurons in rat spinal cord in response to formalin-induced nociception. *Neurosci Lett*. 2000;283(1):29–32. https://doi.org/10.1016/S0304-3940(00)00908-3.
73. Ji RR, Befort K, Brenner GJ, Woolf CJ. ERK MAP kinase activation in superficial spinal cord neurons induces prodynorphin and NK-1 upregulation and contributes to persistent inflammatory pain hypersensitivity. *J Neurosci*. 2002;22(2):478–485. https://doi.org/10.1523/JNEUROSCI.22-02-00478.2002.